

REVERSE MICELLE SYNTHESIS OF NANOSCALE METAL CONTAINING CATALYSTS

John G. Darab, John L. Fulton and John C. Linehan
Pacific Northwest Laboratory¹, Richland, Washington 99352

KEYWORDS: catalyst synthesis, EXAFS, microemulsion

INTRODUCTION

The need for morphological control during the synthesis of catalyst precursor powders is generally accepted to be important. In the liquefaction of coal, for example, iron-bearing catalyst precursor particles containing individual crystallites with diameters in the 1-100 nanometer range are believed to achieve good dispersion through out the coal-solvent slurry during liquefaction runs and to undergo chemical transformations to catalytically active iron sulfide phases².

The production of the nanoscale powders described here employs the confining spherical microdomains comprising the aqueous phase of a modified reverse micelle (MRM) microemulsion system as nanoscale reaction vessels in which polymerization, electrochemical reduction and precipitation of solvated salts can occur. Figure 1 shows a schematic illustration of a typical reverse micelle for the system studied here. The goal is to take advantage of the confining nature of micelles to kinetically hinder transformation processes which readily occur in bulk aqueous solution in order to control the morphology and phase of the resulting powder. A micellar approach to producing nanoscale particles has already been used on a variety of semiconductor, metal and ceramic systems³. The synthetic approach described here is unique, however, in that a much greater yield of powder can be obtained compared to the conventional reverse micelle systems (approximately 10 g/l for the MRM system vs 0.5 g/l for traditional reverse micelle systems).

We have prepared a variety of metal, alloy, and metal- and mixed metal-oxide nanoscale powders from appropriate MRM systems. Examples of nanoscale powders produced include Co, Mo-Co, Ni₃Fe, Ni, and various oxides and oxyhydroxides of iron. Here, we discuss the preparation and characterization of nickel metal (with a nickel oxide surface layer) and iron oxyhydroxide MRM nanoscale powders. We have used extended x-ray absorption fine structure (EXAFS) spectroscopy to study the chemical polymerization process *in situ*, x-ray diffraction (XRD), scanning and transmission electron microscopies (SEM and TEM), elemental analysis and structural modelling to characterize the nanoscale powders produced. The catalytic activity of these powders is currently being studied.

EXPERIMENTAL SECTION

Powder Precursor Salts. Ammonium ferric sulfate dodecahydrate (Fisher) and nickel sulfate hexahydrate (Fisher) were used as-received as precursor salts for iron- and nickel-bearing powders respectively.

Preparation of the Microemulsions (MRMs). In a 2.0-l Erlenmeyer flask 12-gm sodium dodecyl sulfate (SDS) and 80-ml of the 1.0 M aqueous metal salt solution of interest were mixed. To this slurry was added 1-l 0.12 M sodium bis(2-ethylhexyl) sulfosuccinate sodium salt (aerosol-OT or AOT) in isoctane. After rigorous stirring and gentle warming for approximately thirty minutes, an optically transparent microemulsion resulted. Two similar microemulsions were prepared using either 1.0 M aqueous sodium hydroxide or sodium borohydride in place of the metal salt containing solution. Microemulsions were used immediately after preparation.

Preparation of Powders. The nickel metal powder was prepared by adding sodium borohydride MRM to the nickel sulfate MRM slowly with constant stirring. Iron oxyhydroxide powder was similarly prepared by adding sodium hydroxide MRM to the ammonium ferric sulfate MRM. In both cases, after about ten minutes particle formation became apparent as the resulting microemulsion began to change color (from green to black for nickel metal formation, and from yellow/orange to red for iron oxyhydroxide formation) and scatter light. The suspension was then transferred to 500-ml nalgene centrifuge tubes and centrifuged at 6000 RPM for ten minutes. The remaining liquid was decanted off. The compacted powder at the bottom of the centrifuge tubes was then washed and centrifuged in isoctane three times. This was followed by three washings/centrifugings in each of methylene chloride and finally water. Water acidified with HNO_3 was used to wash the nickel powders in order to remove salt byproducts. The wet powders were dried under vacuum at 60°C for 24 hours, then ground in a mortar and pestle.

***In Situ* Study of Particle Formation.** The sodium hydroxide MRM was added to the ammonium ferric sulfate MRM stepwise. After each addition, iron K-edge EXAFS spectra were obtained (see below) from the resulting MRM. Sodium hydroxide MRM was added until the system became translucent as a result of nucleation and precipitation of iron-bearing particles.

EXAFS Measurements and Analysis. Iron K-edge EXAFS spectra were obtained on beam line X19A at the National Synchrotron Light Source, Brookhaven National Laboratory. The data were recorded in a transmission mode using either powders thinly distributed onto cellophane tape, or liquids or suspensions contained in a specially prepared sample cell. For each sample, between three and fifteen scans were recorded and averaged together. Standard EXAFS data analyses were applied to the averaged data to obtain a radial distribution function (RDF)⁴

Additional Characterization of Powders. Scanning and transmission electron microscopies (SEM and TEM) and powder x-ray diffraction (XRD) were performed on the as-prepared powders. A portion of the as-prepared iron oxyhydroxide powder was sent out to a commercial analytical lab (Desert Analytical, Tuscon, Arizona) to be analyzed for Fe, C, S, Na and N.

RESULTS AND DISCUSSION

Nickel Powder. Figure 2 shows an SEM micrograph of the as-prepared MRM nickel powder, indicating that the powder consists of irregularly shaped, sponge-like particles with diameters of 1-10 microns. The particles appear to be aggregates of extremely fine crystallites. XRD analysis confirms the formation of phase-pure nickel metal with an average crystallite size of 12-nm. No oxide phases were detected by XRD. However, energy dispersive spectroscopy (EDS) performed in the scanning electron microscope did detect the presence of oxygen, presumable in the form of a thin oxide layer on the surface of the nickel metal particles. Elemental and BET surface area analyses have not yet been performed on this powder.

The sponge-like morphology of the nanoscale MRM nickel metal powder, which presumably has a high surface area, makes it ideal as a highly dispersible catalyst for various industrial processes. As with most metal surfaces, a ubiquitous metal oxide layer is present on the surface of these nanoscale nickel powders; however, the total oxide content must be less than several weight percent due to the fact that no oxide phases are detected via XRD.

Iron Oxyhydroxide Powder. The dried powder consisted predominantly of irregularly shaped particles with diameters of 1-10 microns. TEM analysis on individual particles reveals no resolvable microstructural features, indicating that the particles are either amorphous or agglomerates of nanometer size crystallites. XRD analysis indicates that the powder has the same diffraction pattern as an iron oxyhydroxide phase typically referred to as two-line ferrihydrite⁵. The elemental analysis of the as-prepared powder shows that it contains 45.62 wt% Fe, 11.62 wt% C, 2.56 wt% S, 0.17 wt% Na and 0.12 wt% N. EDS analysis on the powder confirmed the presence of carbon and sulfur. BET analysis indicates that the surface area of the as-prepared powder is greater than 200-m²/gm.

Aqueous Chemistry of Iron(III) Species. Most 1 M aqueous iron(III) salts in bulk acidic non-complexing solutions contain octahedrally coordinated iron(III)-aquo monomeric complexes, $[\text{Fe}(\text{H}_2\text{O})_6]^{3+}$, in equilibrium with dimeric $[\text{Fe}_2(\text{H}_2\text{O})_8(\text{OH})_2]^{4+}$ and trimeric $[\text{Fe}_3(\text{H}_2\text{O})_9(\text{OH})_4]^{5+}$ species^{6,8}. The addition of base (e.g. NH_3 , NaOH , etc.) to the non-complexing aqueous iron(III) salt solution causes polymerization of the monomeric, dimeric and cyclic trimeric species. In general, polymerization at ambient temperatures occurs via deprotonation of one or two aquo ligands and subsequent olation which forms predominantly edge sharing linkages^{6,7}. Livage *et al.*⁷ discuss the formation of cyclic trimers via the olation of hydrolyzed monomers with dimers. The addition of another monomer yields a planar tetramer. Further olation between tetramers yields double straight-chain polymers.

Under appropriate pH conditions, sulfate ligands can chelate and remain strongly bound to the iron(III) cation even after particle precipitation, giving rise to sulfated iron oxyhydroxides with disordered polymer chains (e.g. kinked- or straight-single chain polymers)^{5,7}. Since the synthetic technique employed here uses sulfate salts, and sulfate and sulfonate containing surfactants, these issues become critical. Chemical and structural analyses of the resulting MRM powders will be used to identify the role of sulfo ligands in the powder preparation process.

The elemental analysis of the as-prepared iron oxyhydroxide powder indicates that an appreciable amount of sulfur has been incorporated into the powder product (iron-to-sulfur molar ratio equals 10.2). Since the elemental analysis also indicates that the molar ratio of carbon-to-sulfur is 12.1 and very little sodium is incorporated into the as-prepared powder, the complexation of the iron(III) cation by dodecyl sulfate groups from the SDS seems most probable. Whether these sulfate groups actually take part in the polymerization reactions occurring in the aqueous cores of the reverse micelles or become associated with the particle surface after precipitation is still uncertain.

Structural Modelling of the Iron-Bearing Powder. Extracting the average number of nearest neighbors from an EXAFS spectrum, especially from those obtained from highly disordered systems (i.e., solutions, suspensions, and amorphous materials) and/or nanometer size grains like those being currently studied, often yields values which are suspect due to structural disorder and Debye-Waller damping⁹. Thus, only comparisons between the various nearest neighbor distances determined from the EXAFS spectra of bulk standards and of *in situ* studies of the MRM system will be considered as valid criteria in trying to elucidate the structure of the iron-bearing particles being formed.

There are primarily seven basic oxide and oxyhydroxide phases of iron which could form under the conditions used in this work: goethite (α -FeOOH), akaganeite (β -FeOOH), lepidocrocite (γ -FeOOH), feroxyhyte (δ' -FeOOH), two-line ferrihydrite (unknown structural formula), six-line ferrihydrite (see below) and hematite (α -Fe₂O₃)⁵.

Goethite, akaganeite and lepidocrocite are all composed of different arrangements of double straight polymer chains connected via corner or edge sharing bonds. The primary structural order in all of these phases, i.e. the bonding in the double straight chains, are identical⁸ and thus yield identical oxygen and iron first nearest neighbor shell radii.

In contrast, feroxyhyte, six-line ferrihydrite and hematite are built up from polymer chains and sheets containing a combination of edge, face and corner sharing linkages, and are thus distinguished from the double straight chain-based phases at the primary structural level. These three phases are all structurally similar in that two layers of the edge, face and corner sharing polymer sheets make up the feroxyhyte structure, while that of the six-line ferrihydrite contains four layers, and that of hematite contains six layers.

In terms of the oxygen and iron first nearest neighbor radii determined using EXAFS then, one can discuss whether the primary structural order of the MRM derived powder is goethite-like or hematite-like. Figure 3 shows the oxygen and iron first nearest neighbor radii determined from the EXAFS RDFs plotted versus the [OH]/[Fe] ratio. Note that as the [OH]/[Fe] ratio increases, the iron first nearest neighbor distance systematically decreases and approaches those representative of bulk phases. This indicates that the iron oxyhydroxide polymers, which may be incorporating some sulfate groups, are becoming larger and more highly condensed. The oxygen nearest neighbor distance initially increases with increasing [OH]/[Fe] ratio but then decreases and eventually approaches those representative of bulk phases. The reason for this behavior in the oxygen nearest neighbor distance is uncertain. After precipitation occurs ([OH]/[Fe] = 2.03) and the resulting powder is washed and dried, the oxygen and iron

first nearest neighbor distances become identical to those found in the goethite phase. We thus conclude that the particles formed in the MRM system are goethite-like in structure.

The XRD pattern for the proto-goethite MRM powder, however, is not representative of bulk goethite but of two-line ferrihydrite, the structure of which is still not well understood. Although two-line ferrihydrite is structurally disordered⁵, its primary structural has been previously investigated using EXAFS^{10,11} and has been shown to be similar to that of goethite¹². We suggest that the iron bearing powder being produced by the MRM process indeed has a goethite-like primary structure but lacks the necessary long-range order observed in bulk goethite, indicating that the particles are extremely small and/or disordered and are most likely in an early stage of development. At such early developmental stages, goethite, akaganeite and lepidocrocite are all structurally identical, i.e., double or disordered double straight polymer chains. Akaganeite and lepidocrocite generally do not form under the conditions used in this work; therefore, as a matter of convenience we have labeled this phase of the as-prepared MRM powder as "proto-goethite".

This proto-goethite structure, which may be related to two-line ferrihydrite, consists of double straight chains or disordered double straight chains with iron and/or oxygen vacancies linked together to form a secondary structure having, at best, limited order. The suggestion that the double straight chains are possibly disordered should not be surprising as it was previously noted that the presence of sulfate anions in the aqueous cores of the reverse micelles could become incorporated into the growing polymer, producing such disordered structures.

SUMMARY

Using a modified reverse micelle process, tens-of-gram per liter quantities of micron sized particles of nanoscale nickel metal and iron oxyhydroxide were produced. The as-prepared nickel metal particles were found to consist of agglomerates of nanometer sized crystallites of nickel having a surface oxide layer. The as-prepared iron oxyhydroxide particles were determined to be either amorphous or agglomerates of nanometer sized crystallites having a structure which is proto-typical to that of goethite.

ACKNOWLEDGEMENTS

This work was supported by the U.S. Department of Energy, Office of Fossil Energy under contract DE-AC06-76RLO 1830 and the Advanced Processing and Technology Initiative.

The assistance of Y. Ma in the collection and analysis of the EXAFS data was most appreciated.

REFERENCES

1. Pacific Northwest Laboratory is operated for the United States Department of Energy by the Battelle Memorial Institute.
2. (a) Pradhan, V.R.; Tierney, J.W.; Wender, I.; Huffmann, G.P. *Energy & Fuels* 1991, 5, 497. (b) Pradhan, V.R.; Herrick, D.E.; Tierney, J.W.; Wender, I. *Energy & Fuels* 1991, 5, 712.
3. Steigerwald, M.L.; Brus, L.E. in *Structure and Reactivity in Reverse Micelles*; Pileni, M.P., ed.; Elsevier: New York, 1989; pp. 189-220.
4. Stern, E.A.; Heald, S. in *Handbook of Synchrotron Radiation*; Eastman, D.E., Farge, Y., Koch, E.E., eds.; North Holland: Amsterdam, 1980.
5. Schertmann, U.; Cornell, R.M. *Iron Oxides in the Laboratory*; VCH: New York, 1991.
6. Flynn, C.M. *Chem. Rev.* 1984, 84, 31.
7. Livage, J.; Henry, M.; Sanchez, C. *Prog. Solid State Chem.* 1988, 18, 259.
8. Baes, C.F.; Mesmer, R.E. *The Hydrolysis of Cations*; John Wiley and Sons: New York, 1976; pp. 226-237.
9. Lee, P.A.; Citrin, P.H.; Eisenberger, P.; Kincaid, B.M. *Reviews of Modern Physics* 1981, 53, 759.
10. Charlet, L.; Manceau, A.A. *J. Coll. Int. Sci.* 1992, 148, 443.
11. Combes, J.M.; Manceau, A.; Calas, G.; Bottero, J.Y. *Geochim. Cosmochim. Acta* 1989, 53, 583.
12. Manceau, A.; Combes, J.M. *Phys. Chem. Miner.* 1988, 283.

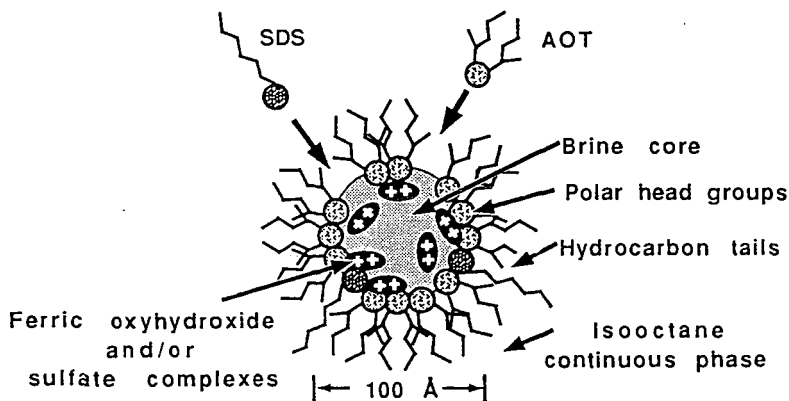


Figure 1. Schematic illustration of a typical reverse micelle for the system studied here.

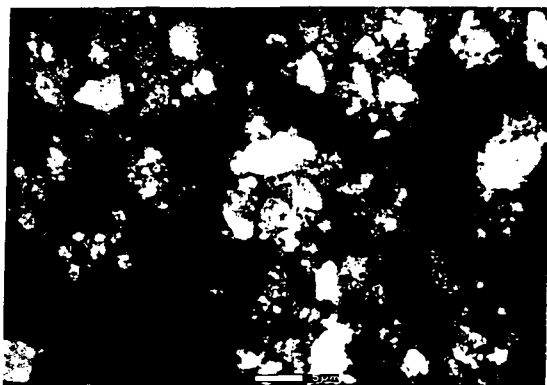


Figure 2. Scanning electron micrograph of the MRM derived nickel metal powder.

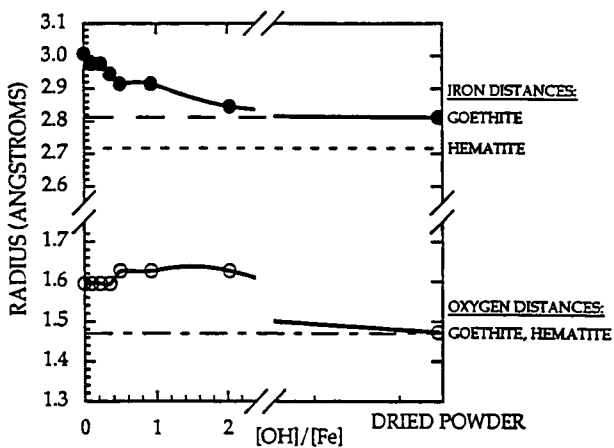


Figure 3. Oxygen and iron first nearest neighbor distances determined from the iron K-edge EXAFS of the ammonium ferric sulfate/ sodium hydroxide MRM microemulsion mixture for various [OH]/[Fe] ratios. Also indicated are the nearest neighbor distances determined for bulk goethite and hematite.